A High-Throughput Computational Study on the Stability of Ni- and Ti-Doped Zr$_2$Fe Alloys

Xin Xie [1], **Xushan Zhao** [2] **and Jiangfeng Song** [3,*]

1 School of Finance, Southwestern University of Finance and Economics, Chengdu 610074, China; 190102@jxycu.edu.cn
2 Computer Network Information Center, Chinese Academy of Sciences, Beijing 100190, China; xushan.zhao@hotmail.com
3 Institute of Materials, China Academy of Engineering Physics, Jiangyou 621908, China
* Correspondence: iterchina@163.com or songjiangfeng@caep.cn

Abstract: Zr$_2$Fe alloys have been widely used in fusion energy and hydrogen energy for hydrogen storage. However, disproportionation reactions occur easily in Zr-based alloys at medium and high temperatures, which greatly reduces the storage capacity of the alloys, and is not conducive to repeated cycle applications. The doping of Zr-based alloys with appropriate transition metal elements has been found to significantly improve their H storage properties and prevent hydrogen disproportionation. A convenient approach is required to efficiently predict the desirable doped structures that are physically stable with optimal properties. In this paper, based on the MatCloud High-Throughput Material Integrated Computing Platform (MatCloud), an automated process algorithm was established to solve the disproportionation reaction of Zr$_2$Fe. Rather than testing the doping materials one by one, such high-throughput material screening is effective in reducing the computational time. The structural stability of modified Zr$_2$Fe alloys, with different doping elements and doping concentrations, is systematically studied. The results indicate that the maximum doping concentration of Ni-doped Zr$_2$Fe is 33 at%, and beyond this doping concentration, Zr$_2$(Fe$_{1-x}$Ni$_x$) phases become unstable. While Ti doping Zr$_2$Fe will form a new phase, the overall hydrogen absorption capacity may have been affected by the decrease in the phase content of Zr$_2$Fe in the main phase. The present study can shed valuable light on the design of high-performance Zr-based alloys for fusion energy and hydrogen storage.

Keywords: metals and alloys; doping; high-throughput screening; first-principles calculations

1. Introduction

With the development of modern society, renewable, reliable, and clean energy are of great significance to maintain the sustainable development of the economy and solve the problem of environmental pollution, especially for China, which is a country with large energy consumption. Among many new energy sources, controlled fusion energy, owing to its safety and high energy density properties, has become one of the ideal ways to solve the energy crisis in the future. In order to realize the great goal of fusion energy power generation, the United States and the Soviet Union proposed carrying out the international thermonuclear experimental reactor (ITER) program in 1985, and then began the design for the ITER in 1998. Since May 2006, China has participated in the ITER program as one of seven international partners. At the same time, in order to bridge the gap between ITER and a demonstration reactor, China has made significant progress in planning for a device called the China fusion engineering test reactor (CFETR), which is a proposed tokamak fusion reactor that uses a magnetic field to confine plasma and generate energy [1].

The deuterium–tritium fusion reaction is a promising way to realize a fusion reaction, which is regarded as the preferred scheme for ITER. Moreover, the tritium fuel cycle system of CFETR is based on a solid breeder blanket design. It not only includes the treatment of the deuterium–tritium fuel gas discharged from the vacuum chamber, and the removal of tritium in the atmosphere and water, but also includes complete breeder tritium extraction, coolant purification, and so on. Since tritium is both a very expensive fuel and a radioactive material, the leakage of tritium will pollute the environment of the fusion reactor. Therefore, the control of tritium is a particularly important issue for a fusion reactor, when using deuterium and tritium as fusion fuels [2].

For the treatment of tritium-containing waste gas, tritium in the glove box is collected in the form of tritium water after catalytic oxidation [3–5]. Now, a large number of tritium-containing waste gas treatment systems, based on catalytic oxidation, exist. However, due to the generation of highly toxic tritium water, such treatment by catalytic oxidation will cause high levels of pollution when running a large amount of tritium. On the other hand, a method based on metal getters, which can capture tritium to form isotopic metal hydrides, is potentially attractive in the treatment of tritium-containing waste gases. The absorption process does not produce tritiated water, and tritium isotopes can also be conveniently recovered via a desorption process. Thus, using metal getters is more feasible and safer for tritium-containing waste gas treatment and tritium storage, and has been vigorously developed by the tritium technology laboratory, aiming at the treatment of tritium in Ci or gram scale. With the development of a magnetic confinement fusion reactor, kg tritium treatment brings new requirements for the improvement of metal getter properties and their interaction with hydrogen isotopes and impurity gases. Systematic study on the doping modification of metal getters is of great significance to improve their performance and application for large-scale tritium treatment in fusion reactors.

As one of the most promising tritium handling and transport materials, the Zr_2Fe alloy is widely used in fusion energy and hydrogen energy for hydrogen storage. The Zr_2Fe alloy has the advantages of fast hydrogen absorption and high absorption efficiency. The equilibrium pressure is 10^{-6} Pa at room temperature, and Zr_2FeH_5 is formed after hydrogen absorption [3]. The Zr_2Fe alloy has high feasibility and safety for hydrogen storage and treatment [4–7]. However, disproportionation reactions occur easily in Zr-based alloys at medium and high temperatures [8–14], which greatly reduces the storage capacity of the alloys, and is not conducive to repeated cycle applications. Hara, M. [8] has conducted a lot of research on the hydrogen-induced disproportionation reaction and its reverse reaction of Zr_2M series alloys. It is found that Zr_2M series alloys can only form stable Zr_2MH_5 (M = Ni, Co, Fe) hydrides in a slower hydrogen absorption state at room temperature. Otherwise, the alloy is prone to disproportionation reactions, especially when the temperature rises to 773 K, when the disproportionation reaction of the alloy will be very fast and the ZrH_2 phase will be formed in tens of seconds. At this temperature, disproportionation of ZrCo, ZrNi and other alloys will also occur, but the reaction rate is obviously slower. The Zr_2Fe alloy is more likely to disproportionate than the other two alloys. Prigent, J. et al. [15] tested the cyclic properties of the Zr_2Fe alloy with pure hydrogen at 0.10 MPa, and found that the hydrogen absorption capacity was obviously affected by the number of cycles used. The first hydrogen absorption capacity is about 1.88 wt%. The second hydrogen absorption capacity is 1.18 wt%. Under the same conditions, the hydrogen absorption capacity of the third cycle is only 0.84 wt%. The change in hydrogen storage capacity can directly reflect the degree of disproportionation reaction. Roupcov, P. [16] also found that the Zr_2Fe-rich phase in the structure is more likely to occur in the disproportionation reaction after hydrogenation of nano-sized Zr-Fe powders. However, it is very time consuming and quite difficult for the experimental methods to obtain exact relative stabilities and hydrogen adsorption configurations for Zr_2Fe alloys.

With the rapid development of computer technology, first-principle methods have become an important tool in exploring the structures and properties of materials [17]. In the past decades, Zr-based alloys have attracted a great deal of first-principle studies. For example, Barberis et al. [18] performed density functional theory (DFT) calculations to estimate the magnetic properties and phase stability of $(Fe, Co, Ni)_{23} Zr_6$ compositions, where the $Fe_{23}Zr_6$ phase has the highest magnetization and the $Co_{23}Zr_6$ phase is the most stable structure for the 23:6 stoichiometry. Then, Ali et al. [19] reported plane-wave-based DFT investigations on the structural, elastic, and lattice dynamical properties of the Fe-rich C15-Fe_2Zr and Zr-rich $FeZr_2$ intermetallic compounds. Both the intermetallic compounds are expected to be thermodynamically and lattice dynamically stable up to 1000 K. Very recently, we studied the electric properties of the gas Fe_2Zr by using the full relativistic theory [20]. The electric dipole moment was found to be symmetrical to the C_{2V} axis of the Zr_2Fe molecule. Moreover, we performed DFT studies on the effects of Hf dopants on helium embrittlement, and the effects of Fe dopants on the hydrogen storage performance of ZrCo materials [21,22]. Thus, employing theoretical calculations is an economical and reliable way to explore the influence of alloying elements on the physical and chemical properties of Zr-based materials, but previous theoretical studies have been restricted to a limited number of doped structures.

In this study, we focus on the stability of the substitutional doping of Ni and Ti into Zr_2Fe, which is expected to improve the anti-disproportionation ability of Zr_2Fe materials [8]. In order to ascertain stable structures, one can calculate the formation energy for each given doping Zr-based compound. However, there are more than ten thousand doped structures for different stoichiometries, from 0 at% to 100 at%. Rather than testing the materials one by one, the simulations need to involve a high-throughput screening computational process. Therefore, based on the MatCloud [23] High-Throughput Material Integrated Computing Platform (MatCloud), a high-throughput and automated process algorithm was established to solve the problem of the disproportionation reaction in the Zr_2Fe alloy. The structural stability of the modified Zr_2Fe alloy with Ni and Ti doping elements and a series of doping concentrations was systematically studied, which may provide a reference for future experimental research.

2. Method and Calculation

The first principle of quantum mechanics and the "cluster expansion" high-throughput screening algorithm, with the MatCloud platform for high-throughput material calculations using systematic research, were carried out to determine the following: (a) Ti replacing Zr in Zr_2Fe alloy; (b) Ni replacing Fe on the structural stability of Zr_2Fe alloy and the possible influence of element alloying on hydrogen adsorption ability.

2.1. Energy Calculation

When calculating the total ground state energy of Zr_2Fe and the doped system, we used the Vienna ab initio simulation package (VASP) program package [24], selected projector augmented wave (PAW) potentials to represent the ionic cores, and used generalized gradient approximation (GGA) with the Perdew–Burke–Ernzerhof (PBE) function [25] to describe electron–ion interactions. The atomic valence configurations of $4s^2 4p^6 4d^2 5s^2$ and $4d75s1$ were considered for Zr and Fe, respectively. The energy cutoff for the plane-wave basis of valence electron wave function is set to 550 eV. A computational model for a $2 \times 2 \times 2$ lattice super cell of Zr_2Fe bulk with 48 atoms was used in the calculations, and the Brillouin zone was sampled with $5 \times 5 \times 3$ Monkhorst-Pack k-point mesh. The tetrahedron method with Blöchl corrections was used to treat partial occupancies and improve the self-consistent field convergence. The Hellman–Feynman force conjugate gradient (CG) algorithm was employed to search the equilibrium position of atoms. The convergence of a self-consistent field was considered sufficient for a total energy difference of less than 10^{-6} eV between iterations, and the force on each atom was converged to 10^{-4} eV/Å during atomic structure optimization.

2.2. Alternative Doping and High-Throughput Screening

Substitution doping is a common method used in material modification research. By substituting one or more points of one or more elements in crystal structure, the effects of different elements/doping concentrations on physical properties of materials are studied. However, there are many ways of substituting doped atoms into the matrix lattice. If one atom is substituted in a supercell of 100 atoms, there will be 100 possible doping structures. Only by first determining the most reasonable structure of doping can the follow-up theoretical calculation or related research be carried out. High-throughput screening typically involves a large number of simulations and a large amount of data management. The cluster expansion (CE) approach is used to speed up the crystal structure screening process, by dividing the structure of a system into groups, such as monomer, two-body, three-body, etc. All these algorithms have been integrated into the high-throughput computational material infrastructure of MatCloud, which provides an effective high-throughput computational infrastructure for integrated management of material simulation, data and resources. Users only need web browsers to set up jobs, submit jobs and perform data management without downloading or installing any software, and without having to worry about computing and data storage issues. As shown in Figure 1, MatCloud provides a high-throughput screening workflow template, which involves procedures of supercell creation, pre-screening for low-energy crystal structures, and calculation of the final properties. The supercell creation procedure generates possible doped structures by traversing all possible replaceable sites. Then, the pre-screening procedure removes the equivalent crystal structures by using a lattice symmetry judgment algorithm, and predicts and screens the low-energy structures using the CE approach. After these high-throughput screening processes, the obtained non-equivalent doped structures are input files for following DFT calculations for geometry optimizations and static calculations for total energies. In this study, we focused on Zr_2Fe-doped materials and provided related algorithms based on the MatCloud platform, as follows:

(1) High-throughput modeling: automatically generated all possible doping structures according to doping concentration, and used a lattice symmetry judgment algorithm to automatically remove equivalent structures;

(2) High-throughput screening: A semi-empirical algorithm based on the CE approach predicted that the formation energy screened the crystal structure and removed the obvious unreasonable structure with high energy. Then, the first-principles calculation of VASP was carried out for the retained structure after primary screening, and the lowest energy was used as the criterion for doping the most stable structure in fine screening.
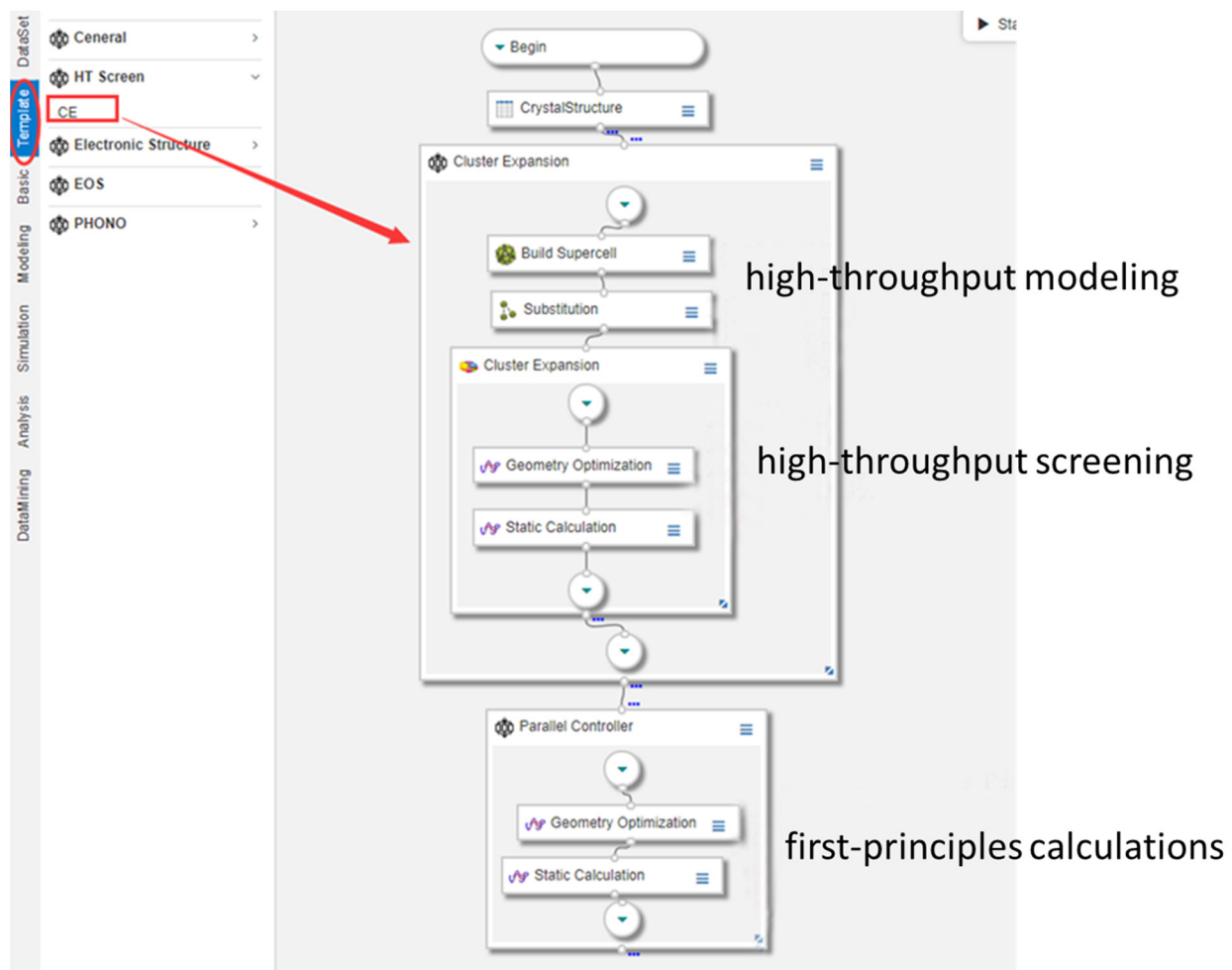
Figure 1. Calculation process for structure screening on MatCloud platform.

3. Results and Discussion

3.1. Crystal Structure and Optimization of Zr$_2$Fe

The crystal structure of Zr$_2$Fe is c (body-centered tetragonal structure, Figure 1), and its space group is I4/mcm. The Zr$_2$Fe crystal cell contains 12 atoms, of which the Zr atom occupies the 4a position and the Fe atom occupies the 8h position. There are two main methods to optimize the lattice constants, which are as follows: (1) all the geometrical parameters of the cell are released to allow free changes in the cell volume, shape and atomic location; (2) based on the original cell, isostatic deformation generates a series of deformed cells of different volumes, and the shape and volume of each deformed cell are fixed separately. Each deformed cell is only allowed to optimize the finite structure by changing the atomic position and obtaining the total ground state energy. The stable structure of the crystal cell can be obtained by fitting to the equation of states (EOS) equation, and so on. In this study, we optimized the crystal structure by fitting to the EOS equation.

Figure 2 shows the change in total energy of Zr$_2$Fe as a function of cell volume. The solid line is the fitting result, according to the EOS of the crystal. The maximum error between the total energy calculation results under different volumes and the fitting results of the equation of state is no more than 3.5×10^{-5} eV, which shows that the above results of quantum mechanics are accurate and reliable, and that the calculation parameters, such as the calculation accuracy, k-lattice and convergence criterion setting in the calculation process, are reasonable. The equilibrium lattice constants of Zr$_2$Fe, obtained by fitting to the EOS equation, are shown in Table 1. The optimized lattice parameters of the stable structure of the Zr$_2$Fe crystal are a = 6.384 Å and c = 5.598 Å, which are in agreement with the experimental values [26] of a = 6.279 Å and c = 5.507 Å, and the previous DFT results [19] of

a = 6.276 and *c* = 5.738 Å. The difference between the calculated lattice parameters and the experimental data listed in Table 1 is <2%. The calculated Wyckoff positions are (0, 0, 0.25) for Fe (4a) and (0.1794, 0.6794, 0) for Zr (8h), which are consistent with the experimental values [26] of (0, 0, 0.25) for Fe (4a) and (0.1728, 0.6728, 0) for Zr (8h). The good consistency between the calculated structural parameters and the experimental values ensures the reliability and accuracy of the calculation method for Zr-based alloys.
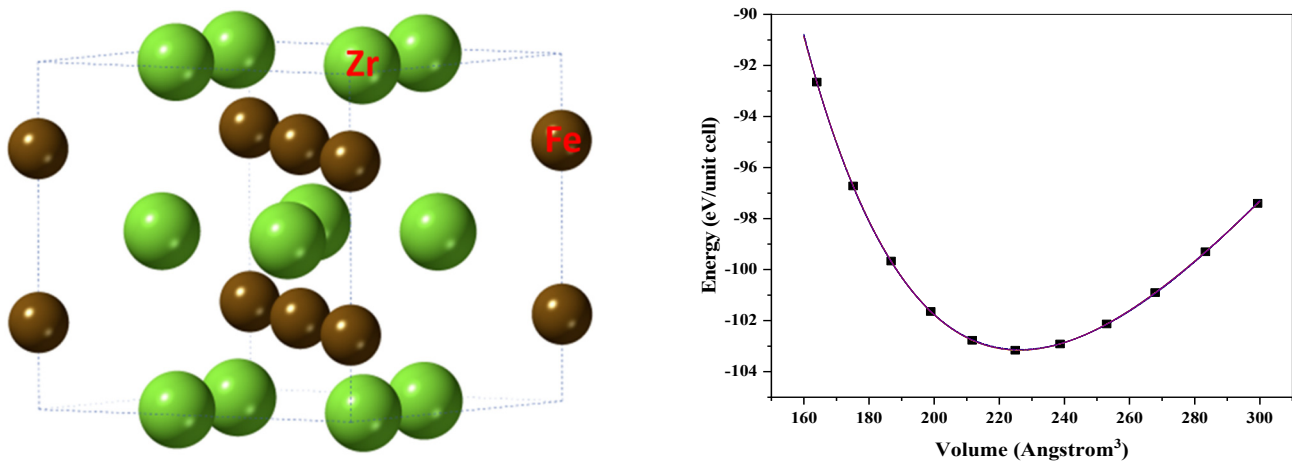
Figure 2. The lattice structure (**left panel**) and the total energy as a function of cell volume (**right panel**) for Zr_2Fe.

Table 1. Calculated cell parameters together with measurements, including lattice parameters *a*, *c* (Å). The fitting errors estimated by |Calc-Expt|/Calc are also shown.

	Calc.	Expt. [26]	Error (%)
a	6.384	6.279	1.64
c	5.598	5.507	1.64

3.2. Structural Stability of Zr_2 ($Fe_{1-x}Ni_x$)-Doped Alloys

Based on the Zr_2Fe cell, the supercell of 2 × 2 × 1 or 2 × 1 × 2 contains 48 atoms, of which 32 are Zr atoms and 16 are Fe atoms. The occupancy fraction (x) of Ni replacing Fe is 0, 1/16, 2/16, 3/16, 4/16, ..., 15/16, 1. High-throughput permutation combination traversal generates a total of 65,536 possible doping structures, and 949 non-equivalent structures, after eliminating the equivalent structures. The 949 non-equivalent structures are predicted by first-principles calculation plus CE approximation. The predicted generation energies for these 949 $Zr_2(Fe_{1-x}Ni_x)$ structures are shown in Figure 3.

In Figure 3, the left side of 0.0 at% is pure Zr_2Fe. With the increase in the x-coordinate value, the content of doped Ni elements increases. Within the range of 2/16~14/16, each doping concentration corresponds to several non-equivalent doping structures. It has been predicted that the most stable structure should have the lowest energy, which can be determined for each doping concentration in Figure 3. On the other hand, only the structures with formation energies below zero are stable and likely to exist in Zr-based alloys; otherwise, there will be a new alloy phase generated, which may reduce the capability of hydrogen absorption in the Zr_2Fe main phase. The following can be observed from Figure 3: (1) the x = 24 at% has the lowest formation energy of −0.017 eV/atom, which is the most favorable doping concentration for $Zr_2(Fe_{1-x}Ni_x)$. (2) Beyond the doping concentration of x = 33 at%, the formation energies are greater than zero and the $Zr_2(Fe_{1-x}Ni_x)$ phase cannot exist stably, which will be unfavorable to the formation of a new phase for hydrogen absorption; thus, the maximum doping concentration of Ni-doped Zr_2Fe is x = 33 at%. (3) Given the atomic radius $R_{Ni} < R_{Fe}$, it can be simply inferred that the stacking gap radius of $Zr_2(Fe_{1-x}Ni_x)$ will be larger than that of Zr_2Fe. The larger gap radius

has been found to be beneficial to the embedding and diffusion of hydrogen atoms [27,28], that is, Ni doping is beneficial to the improvement in hydrogen absorption performance. Therefore, the partial substitution of Fe with the Ni element has a stable $Zr_2(Fe_{1-x}Ni_x)$ phase at low doping concentrations of x < 33 at%, and improves the hydrogen absorption rate of Zr-Fe materials at the primary stage.
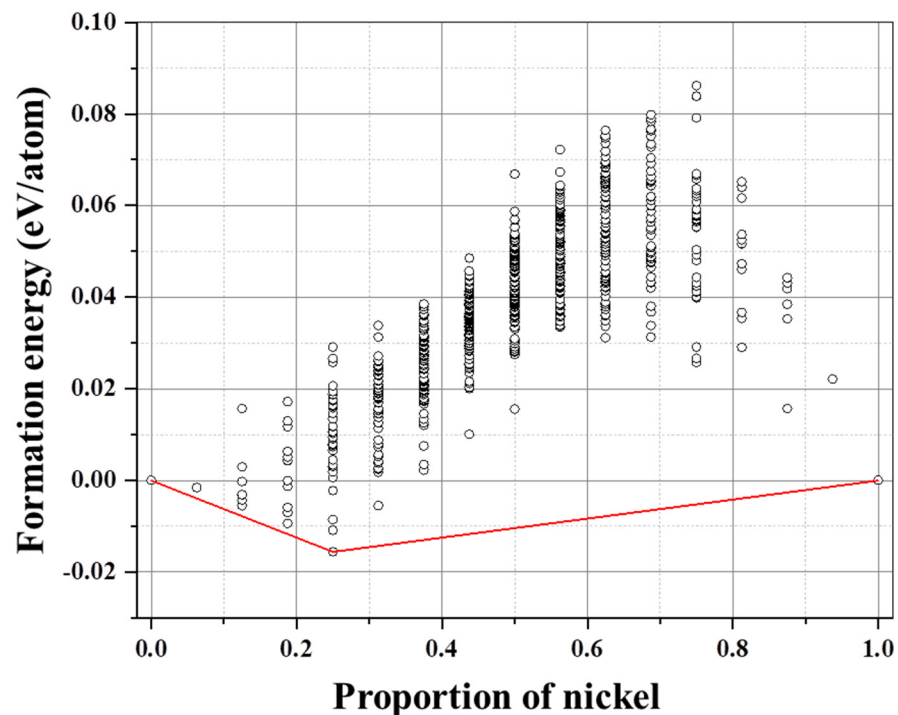

Figure 3. Formation energy of $Zr_2(Fe_{1-x}Ni_x)$ on first-principles calculation plus CE. The red solid line connects the formation energies of x = 0 at% and 100 at% with the minimum value of x = 24 at%.

3.3. Structural Stability of $(Ti_yZr_{2-y})Fe$

There are eight Zr atoms in the cell of Zr_2Fe. Ti atoms are randomly substituted for Zr atoms. According to the amount of substitution, the occupancy fraction (y) of Ti is 0, 1/8, 2/8, 3/8, 4/8, . . . , 7/8, 1, respectively. A total of 256 possible doping structures are generated by high-throughput permutation combination traversal, and 34 non-equivalent structures are excluded. The 34 non-equivalent structures are predicted by first-principles DFT calculations after CE approximation. The predicted generation energies for these 34 $(Ti_yZr_{2-y})Fe$ structures are shown in Figure 4.

It can be observed from Figure 4 that the formation energies of all the non-equivalent $(Ti_yZr_{2-y})Fe$ structures are greater than zero after Ti doping Zr_2Fe. It is difficult to generate doped structures that replace Zr with Ti, which are different to the cases of $Zr_2(Fe_{1-x}Ni_x)$ phases at low doping concentrations of x < 33 at%. In other words, Ti doping Zr_2Fe will deteriorate the lattice stability and new phases may be formed, such as C15-Fe_2Zr- [19] and $Fe_{23}Zr_6$-based alloys [29], with the space groups $Fd\overline{3}m$ and $Fm\overline{3}m$, respectively, resulting in a decrease in the phase content of the main phase Zr_2Fe and affecting the overall hydrogen absorption capacity of the alloy. This result is contrary to the phenomenon of partial Ti substitution for Zr in ZrCo alloys, where Ti doping could significantly improve the lattice stabilities and hydride anti-disproportionation ability of $Zr_{0.875}Ti_{0.125}Co$ [27]. Nevertheless, the effects of doping Ni/Ti on hydrogen absorption and the disproportionation reaction in Zr_2Fe alloys are still in need of further experimental investigations.
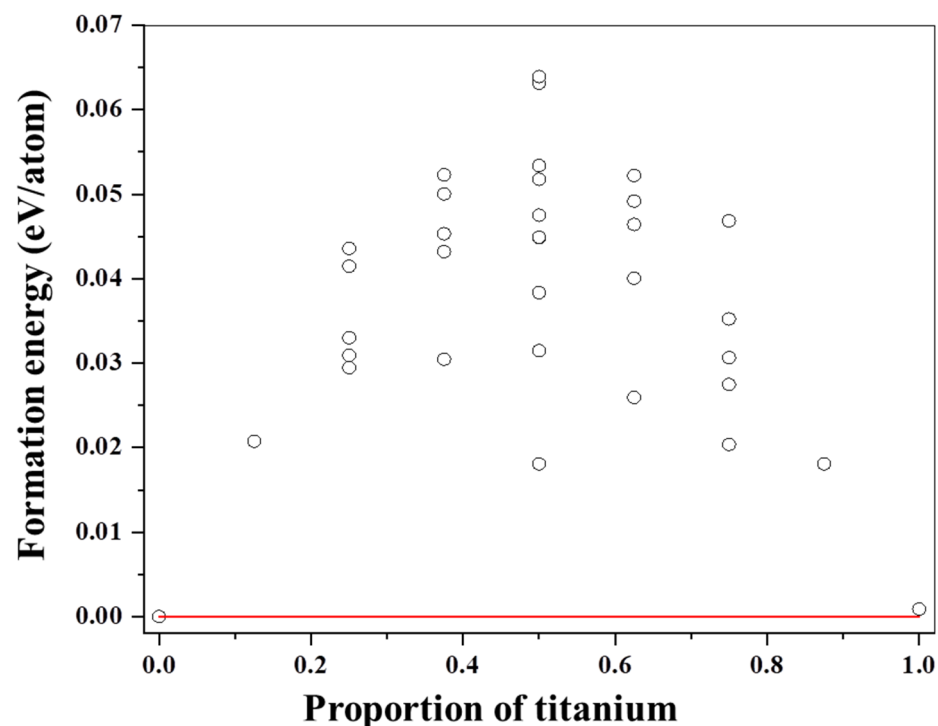
Figure 4. Generation energy of $(Ti_yZr_{2-y})Fe$ on first-principles calculation plus CE. The red solid line represents the zero formation energy.

4. Conclusions

The stability of the substitutional doping of Ni and Ti into Zr_2Fe alloys was studied using first-principle calculations and high-throughput screening. The composition design and scheme optimization through the MatCloud platform can promote the running of large-scale simulations for crystal structure screening and prediction of Zr-based material properties. The replacements of Zr by Ti and Fe by Ni were explored by constructing an automatic calculation flow system. All the possible doping structures were automatically generated according to the doping concentration, and the equivalent structures were automatically removed by using a lattice symmetry judgment algorithm. After this, the semi-empirical clustering expansion approach was used to predict and screen the low-energy structures. Finally, DFT calculations were carried out to optimize the non-equivalent doping Zr_2Fe structure. Rather than testing the doping materials one by one, such high-throughput material screening is effective in reducing the computational time. The main conclusions obtained are as follows:

(1) The maximum doping concentration of Ni-doped Zr_2Fe is x = 33 at%. In view of the atomic radius $R_{Ni} < R_{Fe}$, it can be simply inferred that the stacking gap radius of $Zr_2(Fe_{1-x}Ni_x)$ is larger than that of Zr_2Fe, which is conducive to the embedding and diffusion of hydrogen atoms, that is, Ni doping will be conducive to the enhancement of hydrogen absorption performance.

(2) Ti-doped Zr_2Fe can form a new phase, which results in a decrease in the phase content of Zr_2Fe as the main phase of hydrogen absorption, and further affects the overall hydrogen absorption capacity of the alloys.

(3) Experimental validation after high-throughput computational screening is very necessary, and, reversely, the experimental investigations can improve the performance of high-throughput theoretical algorithms, which is a virtuous circle for designing high-performance materials. Based on this point and our previous studies [30,31], further experimental and theoretical studies of the hydrogen absorption properties of doping Zr_2Fe alloys are still ongoing.

Altogether, we conclude that the composition design and optimization scheme, employing the high-throughput material calculation, can provide a valuable direction for future material design on the basis of experimental verification. The material informatics method has been developed to extensively study the doping modification of Zr-based alloys, which will help to generate a database, screen materials, and explore the application of material information technology. Based on this study, future works on the doping modification of Zr_2Fe alloys with appropriate transition metal elements are expected to include the following aspects: Firstly, one can further explore the effects of both Ti and Ni doping on hydrogen absorption and the disproportionation performance of Zr_2Fe alloys, providing reference for improving the composition design and optimization scheme of high-throughput material calculations. According to the theoretically predicted outcomes of doping modification, systematic experimental studies will be carried out to verify theoretical models and provide a basis for the optimal design of the materials. Secondly, the relationships between macroscopic properties and microstructures, for alloying element substitution and surface modification, will be automatically established by the high-throughput material integrated computing platform. During the search process, the replacement of Zr (by Ti, Hf, Nb and Y) and Fe (by Co, Ni, and Mn) can be systematically studied by an automatic calculation process system. All the possible doping structures are automatically generated, according to the doping concentration, and the equivalent structures are automatically removed by using a lattice symmetry judgment algorithm. The machine learning model will be trained, and then used to predict the generation of irrational structures and remove those with high formation energy. The hydrogen sorption main phase and disproportionated products of Zr_2Fe-based alloys will also be investigated, both theoretically and experimentally. Finally, by carrying out the theoretical predictions of doping elements and concentration ranges that are conducive to stabilizing the main phase of Zr_2Fe hydrogen sorption, inhibiting the formation of the ZrH_2 segregation phase, but stabilizing the Zr_2FeH_5 hydride phase, the types and contents of alloying elements in Zr_2Fe-based materials will be comprehensively evaluated, and the most favorable alloying elements for doping modification will be proposed. All these future works will be beneficial for the development of transition metal-decorated Zr_2Fe materials with high hydrogen storage capacity.

Author Contributions: X.X. conducted all calculations and assisted with data interpretation and preparation of figures. X.Z. and J.S. designed and organized the study and wrote the paper. All authors have read and agreed to the published version of the manuscript.

Institutional Review Board Statement: Not applicable.

Informed Consent Statement: Not applicable.

Data Availability Statement: Not applicable.

Conflicts of Interest: The authors declare no conflict of interest.

References

1. Song, Y.; Wu, S.; Wan, Y.; Li, J.; Ye, M.; Zheng, J.; Cheng, Y.; Zhao, W.; Wei, J.; CFETR Team. Concept design on RH maintenance of CFETR Tokamak reactor. *Fusion Eng. Des.* **2014**, *89*, 2331–2335.
2. Bigot, B. ITER construction and manufacturing progress toward first plasma. *Fusion Eng. Des.* **2019**, *146*, 124–129. [CrossRef]
3. Chattaraj, D.; Majumder, C.; Dash, S. Structural, electronic, elastic and thermodynamic properties of Zr 2 Fe and Zr 2 FeH 5: A comprehensive study using first principles approach. *J. Alloy. Compd.* **2014**, *615*, 234–242. [CrossRef]
4. Cohen, D.; Nahmani, M.; Rafailov, G.; Attia, S.; Shamish, Z.; Landau, M.; Zeiri, Y. Oxidation mechanism of porous Zr_2Fe used as a hydrogen getter. *Appl. Radiat. Isot.* **2016**, *107*, 47–56. [CrossRef] [PubMed]

5. Fukada, S.; Tokunaga, K.; Nishikawa, M. Recovery of low-concentration hydrogen from different gas streams with Zr2Fe particle beds. *Fusion Eng. Des.* **1997**, *36*, 471–478. [CrossRef]

6. Fukada, S.; Toyoshima, Y.; Nishikawa, M. Zr2Fe and Zr(Mn0.5Fe0.5)2 particle beds for tritium purification and impurity removal in a fusion fuel cycle. *Fusion Eng. Des.* **2000**, *49–50*, 805–809. [CrossRef]

7. Nobile, A.; Mosley, W.C.; Holder, J.S.; Brooks, K.N. Deuterium absorption and material phase characteristics of Zr_2Fe. *J. Alloy. Compd.* **1994**, *206*, 83–93. [CrossRef]

8. Hara, M.; Hayakawa, R.; Kaneko, Y.; Watanabe, K. Hydrogen-induced disproportionation of Zr_2M (M = Fe, Co, Ni) and reproportionation. *J. Alloys Compd.* **2003**, *352*, 218–225. [CrossRef]

9. Hara, M.; Hayashi, Y.; Watanabe, K. Temperature driven hydrogen-induced disproportionation of Zr_2Cu. *J. Alloys Compd.* **2009**, *487*, 489–493. [CrossRef]

10. Jat, R.A.; Singh, R.; Parida, S.; Das, A.; Agarwal, R.; Ramakumar, K. Determination of deuterium site occupancy in ZrCoD 3 and its role in improved durability of Zr–Co–Ni deuterides against disproportionation. *Int. J. Hydrogen Energy* **2014**, *39*, 15665–15669. [CrossRef]

11. Jat, R.A.; Singh, R.; Pati, S.; Sastry, P.U.; Das, A.; Agarwal, R.; Parida, S.C. An analogy of interstitial site occupancy and hydrogen induced disproportionation of $Zr_{1−x}Ti_xCo$ ternary alloys. *Int. J. Hydrogen Energy* **2017**, *42*, 8089–8097. [CrossRef]

12. Pang, H.; Li, Z.; Zhou, C.; Wang, H.; Ouyang, L.; Yuan, S.; Zhu, M. Achieving the dehydriding reversibility and elevating the equilibrium pressure of YFe_2 alloy by partial Y substitution with Zr. *Int. J. Hydrogen Energy* **2018**, *43*, 14541–14549. [CrossRef]

13. Yang, G.; Liu, W.; Han, X.; Han, H.; Qian, Y.; Zeng, Y.; Wu, X.; Qiu, J.; Yin, H.; Liu, W.; et al. Effects of alloying substitutions on the anti-disproportionation behavior of ZrCo alloy. *Int. J. Hydrogen Energy* **2017**, *42*, 15782–15789. [CrossRef]

14. Peng, L.; Jiang, C.; Xu, Q.; Wu, X. Hydrogen-induced disproportionation characteristics of Zr(1−x)Hf(x)Co(x = 0, 0.1, 0.2 and 0.3) alloys. *Fusion Eng. Des.* **2013**, *88*, 299–303. [CrossRef]

15. Prigent, J.; Latroche, M.; Leoni, E.; Rohr, V. Hydrogen trapping properties of Zr-based intermetallic compounds in the presence of CO contaminant gas. *J. Alloys Compd.* **2011**, *509*, S801–S803. [CrossRef]

16. Roupcová, P.; Schneeweiss, O.; Zhu, M. Hydrogenation of nanocrystalline Zr-Fe-H powder. *J. Alloys Compd.* **2005**, *404–406*, 537–540. [CrossRef]

17. Burke, K. Perspective on density functional theory. *J. Chem. Phys.* **2012**, *136*, 150901. [CrossRef]

18. Ohodnicki, P.R., Jr.; Cates, N.C.; Laughlin, D.E.; McHenry, M.E.; Widom, M. Ab initio theoretical study of magnetization and phase stability of the $(Fe, Co, Ni)_{23}B_6$ and $(Fe, Co, Ni)_{23}Zr_6$ structures of $Cr_{23}C_6$ and $Mn_{23}Th_6$ prototypes. *Phys. Rev. B* **2008**, *78*, 144414. [CrossRef]

19. Ali, K.; Ghosh, P.; Arya, A. A DFT study of structural, elastic and lattice dynamical properties of Fe2Zr and FeZr2 intermetallics. *J. Alloys Compd.* **2017**, *723*, 611–619. [CrossRef]

20. Song, J.; Zhang, L.; Kong, X.; Hu, X.; Meng, D.; Zhu, Z. Electric Properties of Molecule Zr_2Fe Based on the Full Relativistic Theory. *Molecules* **2019**, *24*, 1127. [CrossRef]

21. Wang, Q.; Kong, X.; Yu, Y.; Song, J.; Wu, L. Influence of the Fe-doping on hydrogen behavior on the ZrCo surface. *Int. J. Hydrogen Energy* **2021**, *46*, 33877–33888. [CrossRef]

22. Kong, X.; Yu, Y.; Shen, Y.; Song, J. Effect of Hf doping on He behavior in tritium storage material ZrCo. *Phys. Chem. Chem. Phys.* **2021**, *23*, 18686–18693. [CrossRef] [PubMed]

23. Yang, X.; Wang, Z.; Zhao, X.; Song, J.; Zhang, M.; Liu, H. MatCloud: A high-throughput computational infrastructure for integrated management of materials simulation, data and resources. *Comput. Mater. Sci.* **2018**, *146*, 319–333. [CrossRef]

24. Kresse, G.; Furthmüller, J. Efficient iterative schemes for ab initio total-energy calculations using a plane-wave basis set. *Phys. Rev. B* **1996**, *55*, 11169–11174. [CrossRef]

25. Perdew, J.P.; Burke, K.; Ernzerhof, M. Generalized gradient approximation made simple. *Phys. Rev. Lett.* **1996**, *77*, 3865–3868. [CrossRef] [PubMed]

26. Raj, P.; Suryanarayana, P.; Sathyamoorthy, A.; Shashikala, K.; Iyer, R.M. Zr2FeHx system hydrided at low temperatures: Structural aspects by Mössbauer and X-ray diffraction studies. *J. Alloys Compd.* **1992**, *178*, 393–401. [CrossRef]

27. Zhang, K.; Wang, F.; Zeng, X.; Zhang, B.; Kou, H. First-principless investigation on the role of interstitial site preference on the hydrogen-induced disproportionation of ZrCo and its doped alloys. *Int. J. Hydrogen Energy* **2020**, *45*, 9877–9891. [CrossRef]

28. Song, Y.; Feng, Y.; Feng, X.; Cheng, Y.; Sun, W.; Pei, X.; Dong, M.; Feng, T.; Qiu, Y.; Wu, C. First-principless study of hydrogen adsorption behavior in C15 Laves phase compound ZrV2. *AIP Adv.* **2021**, *11*, 115010. [CrossRef]

29. Saenko, I.; Kuprava, A.; Udovsky, A.; Fabrichnaya, O. Heat capacity measurement of Zr2Fe and thermodynamic re-assessment of the Fe–Zr system. *Calphad* **2019**, *66*, 101625. [CrossRef]

30. Jiangfeng, S.; Jingchuan, W.; Fei, J.; Peilong, L.; Zhenghe, Z.; Daqiao, M. Experiment and simulation on Zr_2Fe bed for tritium capturing. *RSC Adv.* **2019**, *9*, 1472. [CrossRef]

31. Song, J.; Wang, J.; Hu, X.; Meng, D.; Wang, S. Activation and Disproportionation of Zr_2Fe Alloy as Hydrogen Storage Material. *Molecules* **2019**, *24*, 1542. [CrossRef] [PubMed]